



ELSEVIER

Available online at www.sciencedirect.com

SCIENCE @ DIRECT®

International Journal of Heat and Mass Transfer 48 (2005) 2561–2570

International Journal of
**HEAT and MASS
TRANSFER**

www.elsevier.com/locate/ijhmt

Improvement of a thermal energy storage using plates with paraffin–graphite composite

José M. Marín ^{a,*}, Belén Zalba ^a, Luisa F. Cabeza ^b, Harald Mehling ^c

^a *Dpto. Ingeniería Mecánica, Campus Politécnico, Universidad de Zaragoza Edificio Betancourt, María de Luna 3, 50015 Zaragoza, Spain*

^b *Dpto. d'Informàtica i Enginyeria Industrial, Escola Politècnica Superior, Universitat de Lleida, Jaume II 69, 25001 Lleida, Spain*

^c *ZAE Bayern, Division 1: Energy Conversion and Storage, Walther-Meissner-Str. 6, 85748 Garching, Germany*

Received 8 March 2004

Available online 17 March 2005

Abstract

This work aims at designing a thermal energy storage (TES) using air as heat transfer medium, efficient mainly for free-cooling but also for other applications, improving the low heat transfer rates due to the thermal conductivity of the materials usually employed in these systems, phase change materials (PCM). In this paper, free-cooling means the storage of cold from the night to be used during the day to cool down a room. An experimental set-up has been constructed to simulate the application. The loading and unloading processes (melting and freezing of the PCM) have two disadvantages: a relative long duration, in the range from 3 to 8 h, and a very high power consumption of the fans. Using a porous matrix of graphite where the PCM is embedded, both handicaps can be noticeably overcome. The application is studied, both experimentally and numerically.

© 2005 Elsevier Ltd. All rights reserved.

1. Introduction

The aim of the work is to study the feasibility of a thermal energy system for storing cold from outside air during the night and using it during the day for cooling air or air conditioning. This technology can be used in places where there is a strong difference of temperature between day and night in summer, of at least 15 °C. To get this objective a phase change material, PCM, with a phase change temperature in the middle of the diurnal extreme temperatures is needed and that implies very small temperature differences between the

PCM and the heat transfer medium, air exchanging heat with it. So the enhancement of heat transfer is very important in this application.

Various methods [1] are proposed to enhance the heat transfer in a latent heat thermal storage using water as heat transfer medium, but when air is used as heat transfer medium, the amount of research published is much smaller. Metal matrix structures and finned tubes have been widely used. Satzger et al. [2], Mehling et al. [3–5] and Py et al. [6] proposed a graphite-compound-material, where the PCM is embedded inside a graphite matrix. The main advantage of such a material is the increase in heat conductivity in the PCM without much reduction in energy storage, but other advantages could be the decrease in subcooling of salt hydrates and the decrease of volume change in paraffin.

* Corresponding author. Tel.: +34 976762793; fax: +34 976762616.

E-mail address: jmm@unizar.es (J.M. Marín).

Nomenclature

a	thermal diffusivity ($\lambda_{eq}/\rho c_p$)
A	area
Bi	Biot number
C	volumetric air flow (m^3/h)
c	specific heat for incompressible substances
D_h	hydraulic diameter
e	thickness
f	friction factor
Fo	Fourier number
H	height
h	convection heat transfer coefficient
L	length
m	mass
\dot{m}	mass flow
Nu	Nusselt number
\dot{Q}	heat flow
Re	Reynolds number
T	temperature
t	time
U	internal energy

Greek symbols

ρ	density
λ	thermal conductivity

Subscripts

a	air
env	environment
eq	equivalent
graph	graphite
ins	insulation
i, j	spatial indexes for discretization
m	total spatial intervals in x -direction
n	total spatial intervals in y -direction
p	at constant pressure, temporal index for discretization

Abbreviations

PCM	phase change material
PMMA	polymethylmethacrylate
TES	thermal energy storage

The use of finned tubes has been reported by Morcos [7], Costa et al. [8], and many others; embedding the PCM in a metal matrix structure has been referenced by Kamimoto et al. [9]. Fukai et al. [10] also proposed that the PCM be embedded inside a graphite structure to increase the heat rate without much reduction in energy storage density.

In this paper the technique of using a graphite matrix is used to overcome the low heat transfer rates, because of the following advantages:

- The anisotropy of the graphite allows to address the heat transfer in the direction of interest.
- The graphite matrix occupies only a small space so that the energy storage density remains very close to its value for the PCM alone.
- The matrix introduces no corrosion problems, and
- It's commercially available.

A computer program was made to analyse the operating conditions of the accumulator and an experimental set-up was designed and built to simulate the application and to validate the numerical program.

2. Experimental investigation

2.1. Experimental rig and supporting theory

The experimental rig consists of a close air loop with a storage unit (Fig. 1). The air in the loop can be heated

and cooled artificially. Initially several options for the geometry of the storage were considered, mainly shell and tubes and plates heat exchangers, but in the first ones the melting and freezing process when a PCM alone is found on the outside of the tube surface are not symmetric and so heat transfer is not optimal [11]. This lack of symmetry does not happen when the PCM is embedded in the graphite matrix but, as the aim of the paper is to show the advantages of using this method of increasing the heat transfer rates it's necessary to compare with the case of using PCM alone, the more suitable geometry is taken for both cases, without and with graphite matrices.

Flat plate encapsulates were chosen because of the following advantages:

- The heat transfer in the PCM can be controlled with the choice of thickness of the encapsulation [12].
- Both processes of phase change are symmetric in relation to the two sides of the plates.
- High ratio area/volume: with the geometry used in the experiments, the ratio used was $100\text{--}150\text{ m}^2/\text{m}^3$.
- Less pressure drop in the air.

Using a flat plate encapsulation allows an easy design of the thermal energy storage, as it can be seen in Fig. 2. The external shell was made with plates of polystyrene, with an air chamber in between, to ensure minimum thermal losses. The encapsulation of the PCM was made with polymethylmethacrylate (PMMA) plates to allow

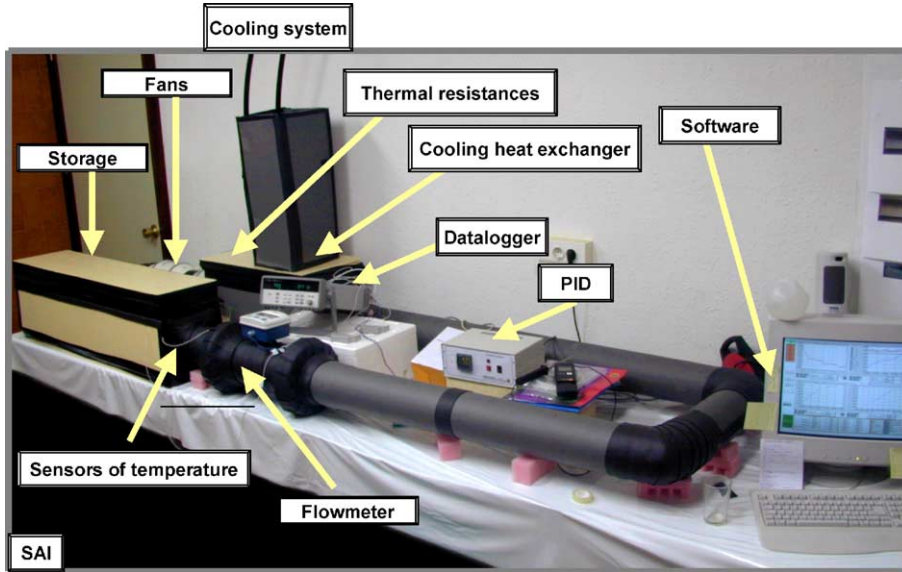


Fig. 1. Picture of the experimental set-up.

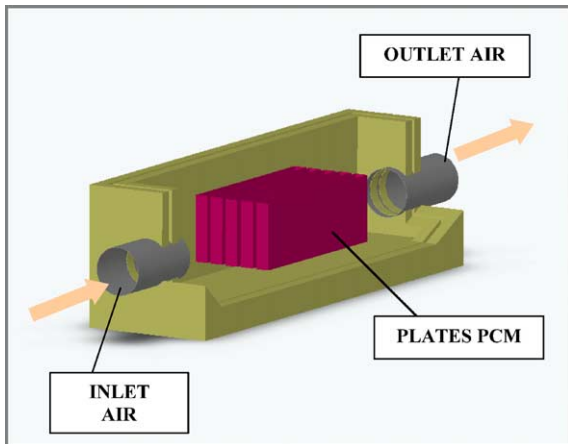


Fig. 2. Configuration of the TES device.

visual observation of the phase change. These plates contain alternatively the PCM alone and the composite with the PCM embedded in a graphite matrix. The size of the plates is 38.5 cm in length, 14.5 cm in height and a thickness of 2.5 cm and their walls have a thickness of 2 mm.

The temperature of the air was measured at the entrance and exit of the storage, using five calibrated Pt100 (uncertainties ± 0.05 °C) in each point; air flow was measured using a calibrated flowmeter (uncertainty <0.5%) [12]. All the data were stored and evaluated with a tailor-made software.

The thermal performance of the thermal energy storage is evaluated with an energy balance:

$$\dot{Q} = \frac{dU_{\text{PCM}}}{dt} = \dot{Q}_{\text{env}} + [\dot{m} \cdot c_p \cdot (T_{\text{inlet}} - T_{\text{outlet}})]_{\text{air}} - \frac{dU_{\text{ins}}}{dt} \quad (1)$$

where $\frac{dU_{\text{PCM}}}{dt}$ is the thermal energy change of the PCM with time; $[\dot{m} \cdot c_p \cdot (T_{\text{inlet}} - T_{\text{outlet}})]_{\text{air}}$ the enthalpy change of the air between its inlet and outlet; \dot{Q}_{env} the heat losses to the environment through the insulating shell, is a small term that can be evaluated with Eq. (2)

$$\dot{Q}_{\text{env}} = \frac{A \cdot \lambda_{\text{ins}} \cdot (T_{\text{wall}} - T_{\text{inside}})}{e} \quad (2)$$

where A is the area normal to heat conduction, T_{wall} and T_{inside} the temperatures of the centre of the internal and external surfaces of the internal plate of polystyrene and e its thickness.

Finally, the last term on the right of Eq. (1) is the thermal storage in the insulating shell. It has also a small value which can be calculated with Eq. (3)

$$\frac{dU_{\text{ins}}}{dt} = \frac{m_{\text{ins}} \cdot c_{\text{ins}} \cdot (T_{i+1} - T_i)}{\Delta t} \quad (3)$$

where $\frac{(T_{i+1}-T_i)}{\Delta t}$ is the numerical derivative of the insulation temperature with time.

2.2. Manufacture of the plates with the composite

The procedure used to make the plates with the composite is the following. The plates containing the composite have an external size of $29 \times 144 \times 384$ mm and the thickness of the walls is 2 mm. The PCM used is commercial paraffin called RT-25 supplied by Rubitherm; the graphite matrix consists of 32 parallelepipedic graphite bars made from the plates provided by SGL-TECHNOLOGIES. With this arrangement, advantage can be taken from the anisotropy offered by the graphite positioning the direction with highest thermal conductivity, about 30 W/m K , coincident with the thickness of the plates, where the heat must flow. It is important too, that this lay out creates films of air between the bars that interrupt the heat transfer in the axial direction, improving the mean temperature difference between the air and the PCM and so the global heat exchanging between them.

The procedure used to embed the PCM into the graphite was melting the paraffin and placing the graphite bars into the liquid PCM, heating at the same time to prevent the solidification of the paraffin; heating has proved to be useful in getting a greater amount of paraffin embedded. The calculation of the fraction of each component in the composite was made by weighing sequentially on a precision balance the empty plates, the plates with the graphite bars and finally the whole set of plates, graphite and PCM embedded. The resulting composition of the composite is shown in Table 1. After the work by Py et al. [6], percentages of the PCM between 65% and 95% are acceptable; in the present work 80% of the paraffin was embedded in the graphite.

2.3. Experimental procedure

The experimental procedure is based on the well known statistical technique called *Design of experiments* (DOE) [13,14]. During the tests, the following operating conditions were used both for the PCM and the composites:

- Temperature of the air: during melting (unloading) of the PCM, the inlet temperature set-point of the air was $30 \text{ }^\circ\text{C}$ and during freezing (loading) was set at

Table 1

Composition of the composite graphite–paraffin

Empty plate weight	290 g
Graphite matrix weight	205 g
Embedded RT-25 weight	801 g
Composite weight	1006 g
Total weight of the plate	1296 g

$16 \text{ }^\circ\text{C}$, representing, respectively, the temperatures of use (indoor air temperature $30 \text{ }^\circ\text{C}$) and of cooling down (loading) the thermal accumulator with cold night air ($16 \text{ }^\circ\text{C}$).

- Air flow: the levels to be used were selected considering the heat transfer rate. Whereas heat transfer in the case of the graphite matrix is thermally controlled basically by the external convection with the air because of the high thermal conductivity of the graphite matrix, in the case of using pure PCM its low thermal conductivity makes competitive the internal conduction resistance and the external convective resistance. A Biot number of about one is recommended [15]. To get such a value the air flows selected were 100 and $150 \text{ m}^3/\text{h}$.
- Initial temperature of the PCM inside the plates: before beginning every test the initial temperature of the PCM must be uniform and stable. For melting this temperature is taken as $18 \text{ }^\circ\text{C}$ and for solidification as $30 \text{ }^\circ\text{C}$, simulating the climate conditions where the accumulator will work.

2.4. Experimental results

To guarantee the quality of the results, replication [14] were made in several cases. In Fig. 3 an excellent agreement can be seen between the three replications performed. Notwithstanding, a careful study of the errors associated with the measurement procedure was carried out from the calibration data of each one of the measuring elements taking part in the tests [16], leading to the absolute and relative values of the uncertainties shown in Fig. 4. For heat exchanged higher than 25 W , where most of the energy is exchanged, the relative errors introduced by the experimental set-up itself are under 1%.

After the eight tests carried out changing the physical quantities mentioned in the previous subsection, Figs. 5 and 6 show the heat transfer measured against time for

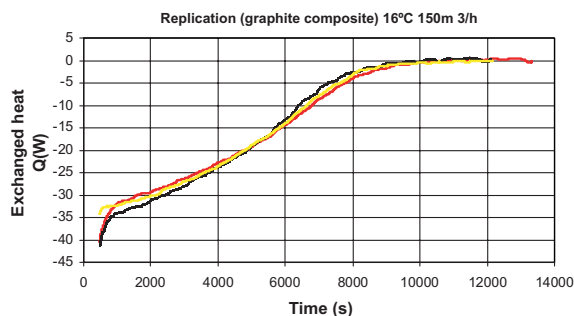


Fig. 3. Replication experiments for solidification with graphite matrix.

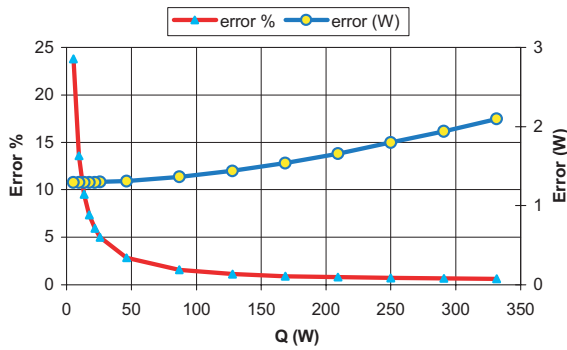


Fig. 4. Uncertainties associated to the experimental installation.

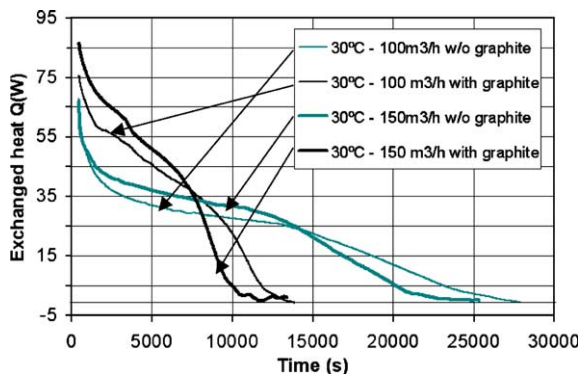


Fig. 5. Exchanged heat by the PCM in melting experiments (encapsulate with and without graphite matrix).

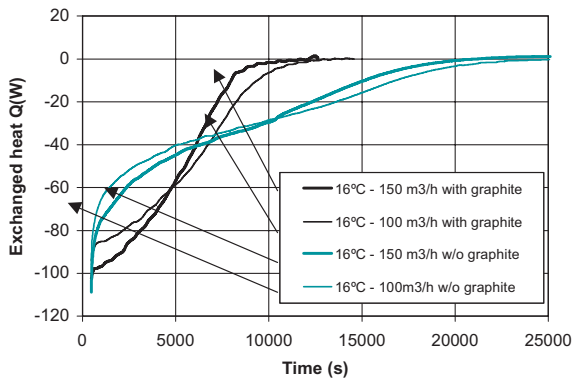


Fig. 6. Exchanged heat by the PCM in solidification experiments (encapsulate with and without graphite matrix).

both kind of plates, those containing the PCM only and the others with the composite. In Table 2 the time taken by the system to reach zero heat exchange between the PCM and the air is indicated for each case and it can be noticed the great reduction of time, about one half,

in the case of using the graphite matrix as compared with the PCM only. Furthermore, the simultaneous very low reduction of the energy stored, between 12% and 20%, as was expected from the storage volume occupied by the graphite.

3. Numerical investigation

In order to analyse possible variations in the performance of the storage under different operation conditions a numerical model is very convenient. A finite difference model can be done in an easy way for the composite and subsequently validated with the experimental results. On the contrary, the big number of complexities arising when the plates are filled only with the PCM, such as viscosity variation with temperature, undercooling phenomena, random character of crystallization, dendritic growth and the creation of holes and cavities [17], make very difficult to elaborate a theoretical model, and the study done here is exclusively experimental.

3.1. Theoretical modelling of the plates with the composite graphite-PCM

The system to be modelized is composed by the PMMA plates containing the graphite matrix embedded with the PCM and the air flow exchanging heat with it. A scheme is presented in Fig. 7.

The numerical modelling of the thermal storage systems (TES) using PCM embedded in a solid matrix is much simpler than in the case of PCM alone because in the first case the main heat transfer mechanism is conduction through the matrix while in the second case the phenomena above mentioned appear.

The numerical model is based on the following assumptions:

- (a) Heat transfer is practically one-dimensional in the direction of the thickness of the plates because of the much greater thermal conductivity in this dimension as explained above, and due to the low conductivity films between the bars.
- (b) The temperature variation of the air flow in the length of the plates is taken into account.
- (c) The symmetry related to a plane in the middle of the thickness of the plates allows to study only the half of each plate.
- (d) Due to the restricted moving capacity of the PCM inside the graphite matrix, convection will not play an important role in heat transfer and so is not taken into consideration [6].
- (e) The energy stored by the PMMA plate walls is neglected. This was foreseen when the system was designed and besides, to check this, a particular test made in the experimental

Table 2

Process time and energy stored for loading and unloading of the accumulator for the PCM without and with a graphite matrix

Type of process	C (m ³ /h)	Process time (h) RT-25	Process time (h) composite	Stored energy (kJ) RT-25	Stored energy (kJ) composite
Solidification	100	6.31	3.16	602	525
Solidification	150	5.47	2.55	600	510.75
Melting	100	7.34	2.83	591	476
Melting	150	6.32	3.47	592	475

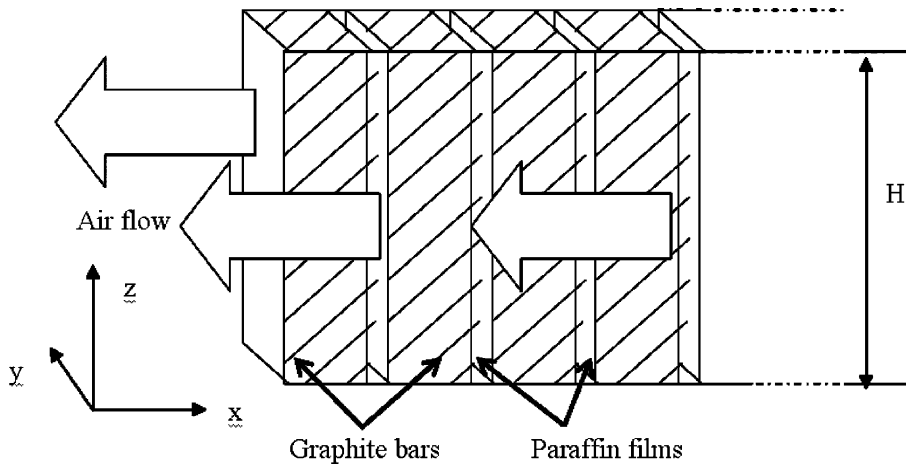


Fig. 7. Coordinates system for the finite difference method.

installation with the empty plates gave a ratio of 2% of stored energy in relation to the plates containing the composite PCM–graphite.

- (f) The thermal conductivity considered is the equivalent in parallel, λ_{eq} , of that of the graphite matrix as given by the manufacturer and that of the air films. The value taken for the graphite matrix is 30 W/m K and the usual value for the air.
- (g) The specific heat of the composite, c_p , is taken as a mass average of the values for the graphite and the paraffin, due to the non-existence of chemical bounds. The value for the paraffin is drawn numerically from the measured enthalpy–temperature curves [12] for the substance used in this study and is shown in Fig. 8. The value for the graphite is well known (709 J/kg K).
- (h) The density, ρ , is calculated as a volume-average of the values of paraffin and graphite. The value for the graphite is well-known and amounts to 2250 kg/m³ and for the PCM the values given by the manufacturer are taken being of 785 kg/m³ for the solid phase and of 749 kg/m³ for the liquid phase.
- (i) Heat losses to the environment are neglected.

The convection coefficient is calculated by means of an appropriate empirical correlation for the non-circular

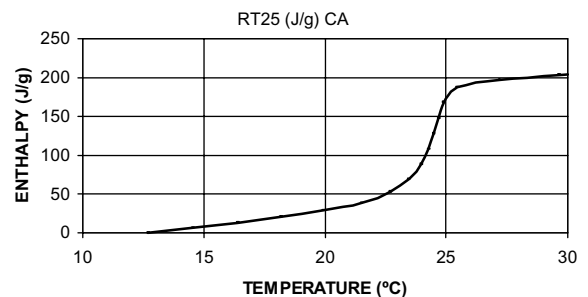


Fig. 8. Enthalpy–temperature curve measured for the RT-25.

duct traversed by the air. Its cross-section is shown in Fig. 9 and its hydraulic diameter is calculated as usually, $D_h = 4A_c/P$, where A_c is the area of the cross-section and P the wet perimeter. The values for this case are $A_c = 0.006429$ m², $P = 1.42$ m and $D_h = 0.01811$ m. Computing the Reynolds number, a transition regime is found where the Gnielinski correlation [18] is adequate:

$$\overline{Nu} = 0.0214 \cdot (Re^{0.8} - 100) \cdot Pr^{0.4} \cdot (1 + (D_h/L)^{2/3}) \quad (4)$$

where L is the length of the channels where the air flows.

A two-dimensional mathematical model can be used, neglecting the heat transfer in the vertical direction. The

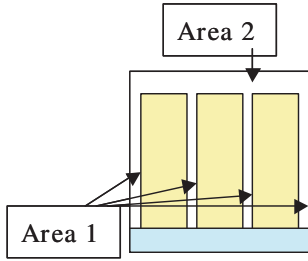


Fig. 9. Cross-section of the thermal storage unit.

graphite matrix must be discretized in their length (x -coordinate) because of the change of the air temperature. A numerical finite difference scheme is used by dividing the plates into cells with dimensions $\Delta x = 11.875$ mm, $\Delta y = 1.2$ mm, $H = 144$ mm in the respective directions of air flow, thickness and height of the plates. Δx is divided into two parts, the first one, 10 mm, is coincident with the length of each individual graphite bar and the rest belongs to the air film. H is the whole height, as this dimension is not discretized.

An energy balance is applied to each of the cells and the following system of equations is obtained in a non-dimensional way:

$$[1 + 2Fo(1 + Bi)]T_{i,1}^p - 2Fo(T_{i,2}^p + Bi \cdot T_{air,i}) = T_{i,1}^{p-1} \quad (5)$$

for the external nodes ($j = 1$),

$$(1 + 2Fo)T_{i,j}^p - Fo(T_{i,j+1}^p + T_{i,j-1}^p) = T_{i,j}^{p-1} \quad (6)$$

for the internal nodes ($j = 2, n - 1$), and

$$(1 + 2Fo)T_n^p - 2Fo \cdot T_{n-1}^p = T_n^{p-1} \quad (7)$$

for the central nodes ($j = n$).

The non-dimensional numbers appearing in the former equations are defined as $Fo \equiv \frac{a\Delta t}{\Delta y^2}$ and $Bi \equiv \frac{h\Delta y}{\lambda_{eq}}$, being $\lambda_{eq} = \lambda_{graph} \frac{\Delta y_{gran}}{\Delta x} + \lambda_{air} \frac{\Delta y_{rim}}{\Delta x} \cong \lambda_{graph} \frac{\Delta y_{gran}}{\Delta x}$. $T_{a,i}$ is the temperature of the air on the node i calculated as:

$$T_{a,i}^p = T_{a,i-1}^p - \frac{q_{i-1}^p}{(\dot{m} \cdot c_p)_{air}} \quad (8)$$

and:

$$q_{i-1}^p = h(\Delta x \cdot H)(T_{a,i-1}^p - T_{i-1,1}^p) \quad (9)$$

As the scheme taken is an implicit one, there are no stability problems in the numerical resolution [19].

3.2. Numerical simulation and validation of the model

To solve the preceding algebraic system of equations a code was programmed using the solver EES [20]. The code was validated simulating the experimentally tested conditions. The comparison is presented in Fig. 10, where the experimental curves do not show the mean

measured values, as usually, but the strip between the higher and lower values determined by the experimental uncertainties mentioned in Section 2.4. It can be seen that the computed values follow exactly the same trend as the empirical ones and are most of the time inside the experimental band. This validation allows that a parametric work can be carried out next with the numerical code to compare alternatives with the case of the plates using the PCM alone.

4. Comparison between the cases of storage without and with the graphite matrix

From the experimental work done in the case of the paraffin alone, the following empirical relations were established between the time of both processes of loading and unloading of the accumulator and the influencing variables [12]. The associated uncertainties are also indicated:

$$t_{solidification} = 5.33 - 0.187 \cdot T - 0.419 \cdot e - 0.0172 \cdot C + 0.0405 \cdot T \cdot e \quad (10)$$

$$\sigma_e^2 = 0.0195$$

$$t_{melting} = -0.59 + 0.186 \cdot T + 2.72 \cdot e - 0.0208 \cdot C - 0.0848 \cdot T \cdot e \quad (11)$$

$$\sigma_e^2 = 0.0092$$

where the range of validity is

for the air temperature [$^{\circ}\text{C}$]:

$$T \in [16 \dots 18 \text{ } ^{\circ}\text{C}]_{\text{solidification}}$$

$$T \in [28 \dots 30 \text{ } ^{\circ}\text{C}]_{\text{fusion}}$$

for the volumetric air flow [m^3/h]:

$$C \in [100 \dots 150 \text{ m}^3/\text{h}]$$

and for the thickness of the plate encapsulates [mm]:

$$e \in [15 \dots 20 \text{ mm}]$$

and the units of the time taken are hours.

From the parametric study done by using the numerical program for the composite graphite–paraffin case, the curves shown in Fig. 11 are obtained. To compare the time reducing effect of the use of the graphite matrix, one representative case for the application considered can be taken. For example in a solidification process by fixing an air temperature of $17 \text{ } ^{\circ}\text{C}$ and a volumetric flow of $100 \text{ m}^3/\text{h}$ from the Fig. 11 the approximate relation (12) is established:

$$t = -0.33 + 0.162e \quad (12)$$

with time and thickness in the same units as before.

Equating the relations (10) and (12), for the values of air and volumetric flow imposed, a relation between the thicknesses of the plates with PCM alone and with the

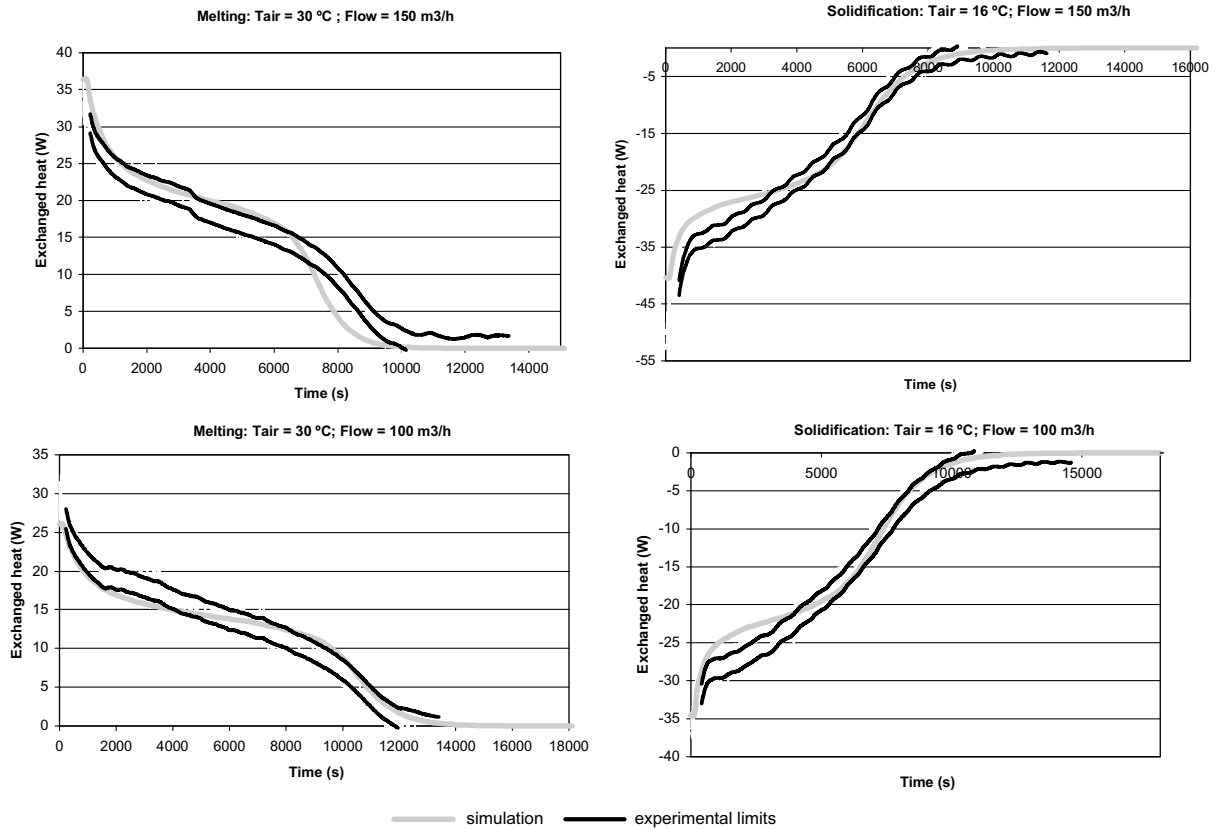


Fig. 10. Comparative curves for numerical and empirical results with the composite.

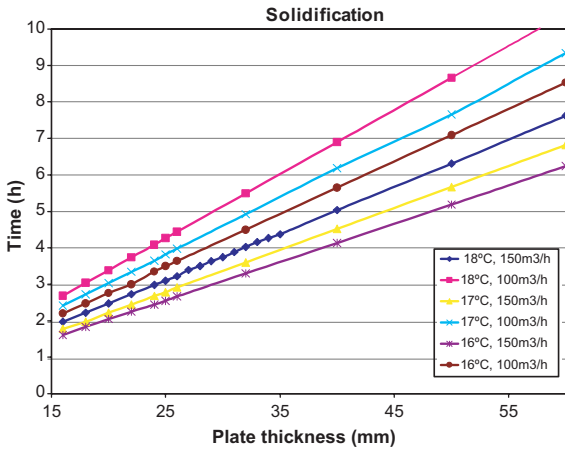


Fig. 11. Computed time versus plate thickness in solidification with the composite.

composite can be derived. Readily it can be seen that the last ones can be 70% thicker for the same time of response, or inversely, with the same thickness a response time much lower can be reached by using the graphite matrix as mentioned in Subsection 2.4.

The former result has several important consequences:

1. The improvement of the thermal conductivity is especially useful in applications in which it is necessary to absorb or release the stored energy in a short period of time. This situation is typical in electronic devices. Also in conventional refrigeration systems where high thermal loads should be evacuated in relatively short intervals of time (restaurants, theatres, cinemas) or in storage systems for hot water.
2. For applications where a reduction of time is not necessary, thicker plates could be manufactured reducing the manufacturing costs, so compensating partially the increase of costs due to the price of the graphite, and besides increasing in the same ratio the width of the channels where the air flows. This implies a significant reduction of the pressure drop and so in the power consumption of the fans used to move the air.

A simple use of the fluid mechanics allows quantifying the range of this reduction. The pressure drop in a flat channel is given by

$$\Delta p = f \frac{1}{2} \rho v^2 \frac{L}{D_h} \quad (13)$$

By using the Blasius expression [21], appropriate for the Reynolds number appearing in the applications considered,

$$f = 0.3164 Re^{-0.25} \quad (14)$$

and considering that for rectangular channels with their width, d , much smaller than the other dimension, as is the case, $D_h \cong 2d$, with the help of Eqs. (13) and (14) it can be concluded that the pressure drop depends on the width of the channel according to the relation $\Delta p \propto d^{-1.25}$. Applying this expression to the increase of about 70% in the width of the channel mentioned above, a reduction of the pressure drop, and so in the fans power consumption, of approximately 50% is reached. As the costs of running the fans are the bigger operating costs and the power consumption is so high [9], this result must not be overridden.

5. Conclusions

Two different cases of thermal energy storage (TES) have been studied, both experimentally and numerically. The study is based on the comparison of the differences of encapsulating in flat plates paraffin alone or embedding it in a graphite matrix to enhance the heat transfer. The paraffin was considered a PCM adequate for the range of temperature handled in the application studied. Excellent agreement of experimental vs. numerical results has been found and a parametric work has been carried out by using the numerical code developed to optimise the system by comparing alternatives.

It has been shown that the second option presents important improvements:

- For the same time of response, the plates could be 70% thicker (inferior costs) and power consumption of the fans decreases by 50%.
- With same thickness for the plates, a response time much lower (50% in time) can be reached with very low reduction of the energy stored (12% and 20%).

Acknowledgements

The authors would like to acknowledge the companies Rubitherm GmbH and SGL TECHNOLOGIES for supplying the materials.

This work was partially funded by the Spanish project DPI2002-04082-C02-01 2003-2005 (Plan Nacional de Investigación Científica, Desarrollo e Innovación Tecnológica 2000–2003), for the Government of Aragón (DGA) and the Research Vicerectorate of the University of Zaragoza.

References

- [1] B. Zalba, J.M. Marín, L.F. Cabeza, H. Mehling, Review on thermal energy storage with phase change: materials, heat transfer analysis and applications, *Appl. Therm. Eng.* 23 (2003) 251–283.
- [2] P. Satzger, B. Exka, F. Ziegler, Matrix-heat-exchanger for a latent-heat cold-storage, in: *Proceedings of Megastock '98*, Sapporo, Japan, 1998.
- [3] H. Mehling, S. Hiebler, F. Ziegler, Latent heat storage using a PCM–graphite composite material: advantages and potential applications, in: *Proceedings of the 4th Workshop of IEA ECES IA Annex 10*, Bendiktbeuern, Germany, 1999.
- [4] H. Mehling, S. Hiebler, F. Ziegler, Latent heat storage using a PCM–graphite composite material, in: *Proceedings of Terrastock 2000—8th International Conference on Thermal Energy Storage*, Stuttgart, Germany, 2000, pp. 375–380.
- [5] L.F. Cabeza, H. Mehling, S. Hiebler, F. Ziegler, Heat transfer enhancement in water when used as PCM in thermal energy storage, *Appl. Therm. Eng.* 22 (2002) 1141–1151.
- [6] X. Py, R. Olives, S. Mauran, Paraffin/porous-graphite–matrix composite as a high and constant power thermal storage material, *Int. J. Heat Mass Transfer* 44 (2001) 2727–2737.
- [7] V.H. Morcos, Investigation of a latent heat thermal energy storage system, *Sol. Wind Technol.* 7 (1990) 197–202.
- [8] M. Costa, D. Buddhi, A. Oliva, Numerical simulation of a latent heat thermal energy storage system with enhanced heat conduction, *Energy Convers. Manage.* 39 (1997) 319–330.
- [9] M. Kamimoto et al. Heat transfer in latent heat thermal storage units using pentarythritol slurry, thermal energy storage, *World Congress of Chemical Engineering*, Tokyo, 1986.
- [10] J. Fukai, Y. Morozumi, Y. Hamada, O. Miyatake, Transient response of thermal energy storage unit using carbon fibers as thermal conductivity promoter, in: *Proceedings of the 3rd European Thermal Science Conference*, Pisa, 2000.
- [11] K.A.R. Ismail, A. Batista, Modeling and solution of the solidification problem of PCM around a cold cylinder, *Numer. Heat Transfer, Part A* 36 (1999) 95–114.
- [12] B. Zalba, Almacenamiento térmico de energía mediante cambio de fase, Tesis doctoral, Zaragoza, Spain, 2002.
- [13] G.E. Box, W.G. Hunteran, J.S. Hunter, *Statistics for Experimenters. An Introduction to Design, Data Analysis*, Wiley, New York, 1999 (Chapter 10).
- [14] R. Mason, R. Gunst, J. Hess, *Statistical Design and Analysis of Experiments*, Wiley, New York, 1989, Chapters 7 and 9.
- [15] N. Shamsundar, E.M. Sparrow, Effect of density change on multidimensional conduction phase change, *J. Heat Transfer, Trans. ASME* 98 (1976) 550–557.
- [16] Standard EAL-G23, The expression of uncertainty in quantitative testing, *European Cooperation for Accreditation of Laboratories*, 1996.

- [17] M. Costa, A. Oliva, C.D. Pérez Segarra, R. Alba, Numerical simulation of solid-liquid phase change phenomena, *Comput. Meth. Appl. Mech. Eng.* 91 (1991) 1123–1134.
- [18] V. Gnielinski, New equations for heat and mass transfer in turbulent pipe and channel flow, *Int. Chem. Eng.* 16 (1976) 359–368.
- [19] G. Myers, *Analytical Methods in Conduction Heat Transfer*, 199, AMCHT Publications, USA, 1998, Chapter 8.
- [20] S.A. Klein, *Engineering Equation Solver (EES), F-Chart Software & McGraw-Hill*, 2003.
- [21] F. White, *Mecánica De Fluidos*, McGraw-Hill, México, 1979 (Chapter 6).